Numerical analysis and combustion control of Shenmu pulverized semi-coke

Guan-Fu Pan, Zhi-Qiang Gong, Zhi-Cheng Liu, Hong-De Xia, Zhen-Yu Tian*

Institute of Engineering Thermophysics, Chinese Academy of Sciences, Beijing, China

Abstract

The combustion characteristic of Shenmu pulverized semi-coke (SSC) was comprehensively investigated with an online TG-FTIR-MS system. The results indicate that the increase of total flowrate, decrease of particle size and heating rate lead to lower ignition, burnout temperature and activation energy. Lower concentration of pollutants such as NO and NO_2 were observed at slower heating rate and larger total flowrate, while their production is insensitive to the particle size. These results are useful in understanding the combustion process of SSC and controlling the formation of pollutants.

1. Introduction

The semi-coke was made from pyrolysis of bituminous coal. It is well known that semi-coke has high fixed carbon and chemical activity and contains low aluminum, phosphor and sulfur. In the past few decades, the semi-coke made from Shenmu bituminous coal (SBC), which has huge reserves, has been extensively used in China. The research focused on the combustion characteristics of Shenmu semi-coke (SSC) is extremely important for its application.

Several studies have been reported previously on the characteristics of SSC burning and gasification. Wang et al. investigated the characteristics and activation of CO_2 in the combustion of SSC (pyrolyzed at 500 and 700 ^oC) [1]. The activation reactivity with CO_2 of semi-coke were found in the order of vitrinite > inertinite [1]. Zhang et al. used distributed activation energy model (DAEM) to study the oxidation behavior of the three kinds of semi-coke including SSC in the chemical reaction controlling regime. The results indicated that DAEM could successfully describe the change of activation energy with the weight loss of semi-coke during oxidation [2]. With thermogravimetric (TG) analysis, Zhao et al. studied the ignition temperature (T_{ig}), maximum reaction temperature (T_{max}), burnout temperature (T_{burn}), burning rate and combustion features of Shenmu coal and SSC mixed sample [3]. The results showed that with the increasing of the SSC content, T_{ig} of the coal and SSC mixture, the caloric value of the sample and the T_{max} would increase, while the burning rate would decrease [3]. Liu et al. investigated the combustion characteristics of SSC prepared by plasma gasification [4]. The results showed that the combustion of SSC could occur steadily in the fluidized bed and the combustion products could steadily release. The activation energy of SSC was observed to be higher than that of the raw coal and its reaction activity was lower than that of the coal [4]. Moreover, Guo et al. studied the CO_2 reforming of methane over SSC and concluded that SSC could be used as a stable catalyst [5]. Compared to these results, the understanding of detailed kinetics concerning the effect of the particle size, heating rate and total flowrate on SSC combustion is limited.

The present work aims to reveal the combustion characteristics of SSC with a newly developed TG-MS-FTIR method. The characteristic temperatures, activation energies and products are deduced. An attempt to correlate the features with the nature and experimental conditions will be discussed.

2. Materials and methods

2.1 SSC samples

The SSC samples were produced at the temperature 600-700 ^oC by the pyrolysis of SBC which was bought from Shenmu Energy Developments Ltd Company. The SSC samples were firstly grinded to small particles and were sieved to diverse particle sizes of < 40, 90-100, 128-180, 280-355 and 355-500 μm. In order to remove the moisture in SSC samples, the samples were put into a drying oven at 105 ℃ for more than two hours. The phases of SSC samples were measured by Bruker D8 Focus X ray diffraction (XRD) with Cu Kα radiation, scan angle of 5-90^o and scanning step of 0.02^o. The XRD results show that the SSC samples are mainly composed of $CaCO_3$, SiO_2 and Kaolinite, as shown in Fig. 1.

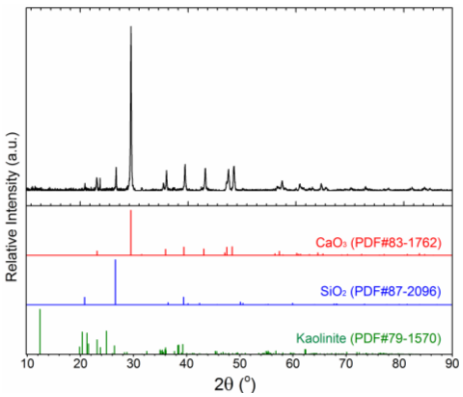

Fig. 1 XRD patterns of SSC samples.

The elements of SBC and SSC samples were identified by the coal proximate analyzer as shown in Table 1. The M_{ad}, A_{ad}, V_{ad}, and F_{Cad} represent the moisture, ash, volatile, and fixed carbon, respectively.

* Corresponding author: tianzhenyu@iet.cn

The C_{ad}, H_{ad}, O_{ad}, N_{ad} and S_{ad} represent carbon, hydrogen, oxygen, nitrogen and sulfur elements in in air dried basis, respectively. M_{ad}, A_{ad}, and F_{Cad} all decreased, and V_{ad} increased after the pyrolysis process. From SBC to SSC, all the elements decline except for C_{ad} through pyrolysis [6].

Table 1 The proximate and ultimate analysis results of SBC and SSC

Name	Proximate analysis				Ultimate analysis				
	M_{ad}	A_{ad}	V_{ad}	F_{Cad}	C_{ad}	H_{ad}	O_{ad}	N_{ad}	S_{ad}
SBC	11.80	9.82	30.57	47.80	62.94	3.88	10.18	1.98	0.40
SSC	14.60	11.36	7.32	66.72	68.31	0.85	4.01	0.58	0.30

2.2 Comprehensive test

A combined TG-MS-FTIR system comprising a TG analyzer (STA-449F3, Netzsch), a mass spectrometer (QMS403C, Aeolos) and an FTIR spectrometer (Tensor 27, Bruker) was used to study the combustion characteristics of SSC. As displayed in Fig. 2, the data measured in the TG-MS-FTIR system were recorded simultaneously by a computer.

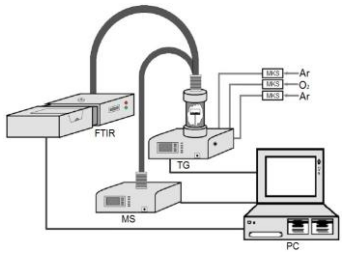

Fig. 2 Schematic diagram of TG-MS-FTIR system.

About 10 mg SSC sample was dispersed on the alumina pan and the atmosphere in TG chamber was replaced with a gas mixture which consists of 20 % O_2 and 80 % Ar. The oxygen content is similar to the air and much more than the theoretically needed for the complete oxidation of the SSC sample. The SSC samples were heated with a heating rate of 10 ℃/min from 40 to 110 ℃ and kept for 30 min. The samples were heated to 1200 ℃ by four kinds of heating rates, namely 10, 20, 30 and 40 ℃/min. During the whole heating processes, three total flowrates (50, 100 and 150 sccm) containing 20 % O_2 and 80 % Ar were used to evaluate the effect of flowrate on SSC combustion. The detailed experimental conditions are shown in Table 2.

Table 2 Experimental conditions

No	Mass (mg)	Flowrate (sccm)	Heating rate (℃/min)	Particle size (μm)
1	10.044	100	20	0-40
2	10.617	100	10	90-100
3	9.298	100	20	90-100
4	9.445	100	30	90-100
5	9.191	100	40	90-100
6	10.300	100	20	125-180
7	9.910	100	20	280-355
8	9.145	100	20	355-500
9	9.855	50	20	90-100
10	9.465	150	20	90-100

2.3 Analysis

2.3.1 Characteristic temperature

The combustion characteristics of semi-coke are usually identified by the T_{ig}, T_{max} and the burnout temperature (T_{burn}). In this work, T_{ig} was obtained with the commonly recognized TG-DTG method [7]. T_{burn} is defined as the temperature with 98% total weight loss. T_{max}, referring to the temperature at which combustion product own maximum volumetric flow, was also determined through numerical analysis.

2.3.2 Kinetic analysis

The kinetic parameters of SSC combustion were calculated by the most widely used Coats-Redfern method [8]:

$$n=1,\quad \ln\left[\frac{-\ln(1-\alpha)}{T^2}\right]=\ln\left[\frac{AR}{\beta E}\left(1-\frac{2RT}{E}\right)\right]-\frac{E}{RT} \quad (1)$$

$$n\neq 1,\quad \ln\left[\frac{1-\ln(1-\alpha)^{1-n}}{T^2(1-n)}\right]=\ln\left[\frac{AR}{\beta E}\left(1-\frac{2RT}{E}\right)\right]-\frac{E}{RT} \quad (2)$$

where $\alpha=(m_0-m)/(m_0-m_\infty)$ refers to the weight loss ratio; m, m_0 and m_∞ represent the sample mass, initial mass and the final mass, respectively; β is heating rate, K·min^{-1}; R is the gas constant and E stands for activation energy, J·mol^{-1}; A is the frequency factor, min^{-1}; n refers to the order of reaction. Due to the item $\frac{2RT}{E}<<1$ and $(1-\frac{2RT}{E})\approx 1$, the first item of the right side of equations is estimated to be a constant. E can be determined from the slope by plotting the item of the left side and [-1/(RT)].

2.3.3 Products

Both MS and FIIR were used to perform the quantitative analysis of the volumetric flowrates of the combustion products. In this work, the MS results were analyzed by a novel method of equivalent characteristic spectrum analysis and the details of this method can be found elsewhere [9]. In the MS analysis, argon was used as a reference gas to calibrate the products. By considering the ion flow intensities, electron impact ionization cross sections and the partial pressures of different species, the volumetric flowrates and relative sensitivity were deduced. In order to exclude the effect of initial coal weight on the formation of products, the initial weight of SSC samples were normalized.

Since the mass loss of sample mainly comes from the decomposition of volatiles in the coal samples, the DTG results measured by TG analyzer agree well with the calculated DTG results from MS measurements. The DTG curves calculated from MS results and measured TG results under condition 4 (see Table 2) are shown in Fig. 3 as a representative. The result illustrate that the calculated MS results agree well with the measured one and the relative uncertainty was estimated to be 0.059 [9].

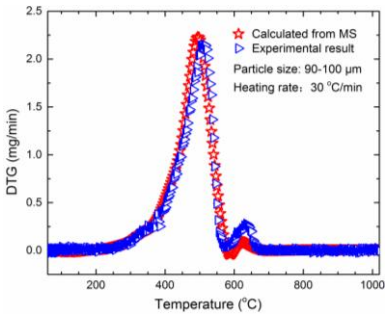

Fig. 3 Comparison of DTG curves from calculation and experiment.

3. Results and discussion

3.1 TG/DTG results

Figure 4 displays the TG/DTG curves of SSC combustion. As shown in Figs. 4a and 4d, the maximum weight loss is observed to increase slightly as the particle size increses from less than 40 to 355 μm and then decrease up to 355-500 μm. The combustion rate depends on both diffusion and reaction ability [10]. If the size of SSC particles were small enough and the quantity of supplied oxygen is much more than that of the theoretical needed for the complete combustion, the effect of diffusion which is determined by energy transfer is insignificant in the combustion processes[11]. Thus, the reaction ability of combustion is expected to play a crucial role. As bigger particle sizes exhibit larger fuel density and less hollows, the reaction ability would be better with bigger particle size than that of smaller ones. When the particle size turns big enough, the diffusion ability becomes gradually the key factor for SSC combustion. In this work, the SSC combustion gets more difficult with particle size bigger than 355 μm, which is responsible for the decline of weight loss in the DTG curves with particle size of 355-500 μm.

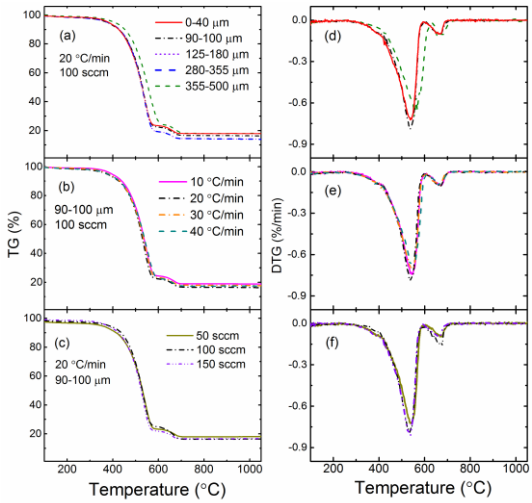

Fig. 4 TG and DTG curves of SSC combustion.

Figures 4b and 4e show the TG and DTG curves of SSC combustion with four heating rates, respectively. The results suggest the SSC combustion be insensitive to the heating rate but with a slight increase at 20 ^{o}C/min. Compared to effect of the heating rate, total flowrate has more clear effect, as shown in Figs. 4c and 4f. As the total flowrate increases, the peak of weight loss moves towards lower temperatures. In addition, the peak value increases as well. Since diffusion ability is the dominant factor in affecting the combustion during rapid combustion process, larger total flowrate leads to more oxygen contact with the sample surface. This would make the combustion occur easily, which generally leads the maximum weight loss to peak at lower temperature and the peak value to increase.

3.2 Characteristic temperatures

The characteristic temperatures are summarized in Fig. 5. As indicated in Fig. 5a, T_{ig}, T_{max} and T_{burn} tend to fall down when the particle size decreases. This is mainly due to the larger surface area exposing to oxygen with smaller particle size [12]. Figure 5b presents the characteristic temperature influenced by heating rate. As the heating rate decreases, the T_{ig}, T_{max} and T_{burn} are observed to decrease slightly. This is due to the fact that the SSC particle has better thermal conduction and energy transfer at lower heating rate than that at higher ones. The diffusion becomes better with higher thermal conductivity, which will benefit to the devolatilization and results in lower T_{ig}. Moreover, the reaction time is more sufficient at lower heating rate [13]. Considering the developed pore structures of SSC, it is more difficult to form ash cladding with slower heating rate which will plugging the surface pores. For this reason, the T_{burn} turns lower [14-17]. As far as the total flowrate is concerned, slight decrease of T_{ig}, T_{max} and T_{burn} are observed with large total flowrate (see Fig. 5c). Since more oxygen comes from the larger total flowrate, the contact of oxygen and the samples surface turns easiser and the ignition and burnout of SSC occur at lower temperature.

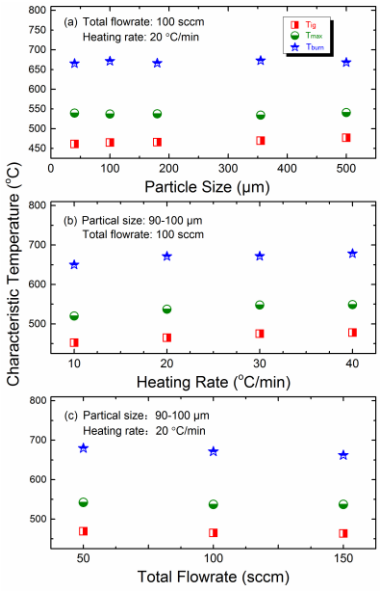

Fig. 5 Characteristic temperatures of SSC combustion.

3.3 Activation energy

Figure 6 depicts the *E* of SSC with variation of particle size, heating rate and total flowrate. The change tendency of *E* is the same as that of characteristic

temperature. *E* tends to be small with the decrease of particle size and heating rate. But when the total flowrate turns large, *E* will turns small. As the particle size decreases, the surface area increases, which would result in more contact area with oxygen and better thermal reactivity. Thus, energy transfer from outside into inner becomes more rapidly, and *E* is getting lower. Since the micropore amount and pore volume of SSC is much more than that of SBC, the adsorptivity of oxygen will also turns better after pyrolysed from parent coal. The influence of energy transfer plays a more significant role in the combustion of SSC than that of SBC. With slower heating rate, the heating time turns longer and the heat transfer rises, which could lead to better diffusion [18]. The oxidation of SSC particles will also turns easier. When the total flowrate rises from 50 to 150 sccm, more oxygen molecules are adsorbed on the surface of samples and make the combustion easy to happen.

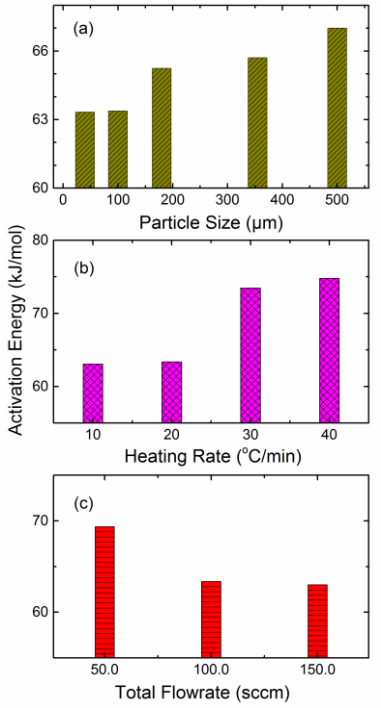

Fig. 6 Activation energies of SSC combustion.

3.4 MS and FTIR results

With MS and FTIR analysis, 14 speices were quantified in this work, including CO, CO_2, H_2, H_2O, nitrogeneous and sulferic compounds. As representatives, Table 3 summarizes the maximum volumetric flowrates of CH_4, NH_3, NO, HCN, NO_2 and SO_2 as well as the corresponded temperatures (T_{max}). By comparing the results obtained at different particle size, the combustion products are insensitive to particle size. In view of the heating rate, lower amount of NO, NO_2 and SO_2 were measured at lower heating rate. In addition, when the heating rate turns faster, the temperature of these maximum volumetric flowrate located at lower temperature. As far as the total flowrate is concerned, the quantity of NO_2, HCN, SO_2 and NH_3 becomes lower when the total flowrate is larger. Moreover, the temperature with maximum volumetric flowrates of NO_2, HCN, SO_2 appear at higher temperature when the total flowrate turns larger. T_{max} refers to the temperature at which the peak flow is obtained.

Considering the environment pollution, the releasing level of nitrogen oxides is the main focus. Figure 7 shows the volumetric flowrates of NO and NO_2 during the combustion process of SSC. The nitrogen components enriched in char will release to form NO and NO_2 during the rapid combustion of char [19]. By comparing the volumetric flowrate peaks of NO and NO_2 it can be found that the production of NO and NO_2 are insensitive to the variation of particle size. It can be easily found that less NO and NO_2 were produced with lower heating rate and larger total flowrate. This could result from the contact time and enough oxygen under such conditions. The results indicate that slower heating rate and larger total flowrate conditions will help to control the pollution from SSC combustion.

FTIR with the spectral range of 500-5000 cm^{-1} was involved in the current work to visualize the formation of the major species and avoid the effect of ion fragmentation in MS. Figure 8 presents the three-dimensional spectra measured with the limited conditions. The maximum absorbance peak is located at

Table 3 Maximum volumetric flow of products

No	CH_4		NH_3		NO		HCN		NO_2		SO_2	
	Value (slm)	T_{max} (℃)	Value (slm)	T_{max} (℃)	Value (slm)	T_{max} (℃)	Value (slm)	T_{max} (℃)	Value (slm)	T_{max} (℃)	Value (slm)	T_{max} (℃)
1	3.58E-04	535	2.95E-03	537	1.51E-04	534	2.57E-04	514	7.73E-05	503	4.34E-05	539
2	5.32E-05	509	1.36E-04	533	8.99E-05	530	5.97E-04	510	4.70E-05	510	6.48E-06	541
3	5.75E-04	532	1.07E-03	536	1.04E-04	530	2.57E-04	516	8.35E-05	509	4.75E-05	541
4	4.34E-04	443	7.68E-03	555	1.05E-04	524	1.85E-04	511	1.29E-04	495	9.47E-05	507
5	4.45E-05	520	1.09E-04	470	1.37E-04	520	4.26E-04	488	1.45E-04	488	9.26E-05	511
6	2.73E-05	530	2.28E-04	526	8.53E-05	536	2.23E-04	526	1.09E-04	513	1.01E-05	555
7	4.07E-05	530	1.19E-04	488	1.07E-04	532	4.35E-04	511	9.90E-05	511	1.33E-05	536
8	4.54E-05	522	7.27E-05	508	1.56E-04	540	3.76E-04	508	7.20E-05	512	5.37E-05	523
9	2.40E-04	554	3.17E-03	554	2.18E-04	544	4.97E-04	536	1.66E-04	507	5.73E-05	540
10	1.42E-04	528	2.97E-04	635	1.14E-04	529	1.08E-04	514	5.70E-05	521	3.08E-06	567

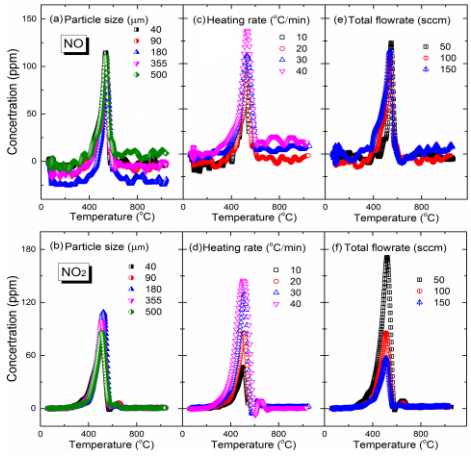

Fig. 7 Concentration of NO and NO_2 during combustion.

the wavenumber of 2380 cm^{-1} corresponding to the overlap of anomalistic vibration of CO_2 and CO. The second obvious peak at 700 cm^{-1} belongs to the bending vibration of CO_2. By comparing the second obvious peak value relative to the maximum absorbance peak value, the percentage of the CO_2 can be deduced. From the spectra shown in Fig. 8, bigger particle size, slower heating rate and larger total flowrate generally leads to more complete oxidation of SSC.

By comparing the standard spectra of specific species, overlapped peaks were observed. For instance, the peak at 1500-1800 cm^{-1} contains the contributions of both H_2O and NO [20,21]. As can be seen in Fig. 8, CO_2 becomes detectable at around 140 ℃. Up to 200 ℃, a slow increase was observed. The fast production of the major species was achieved within the temperature

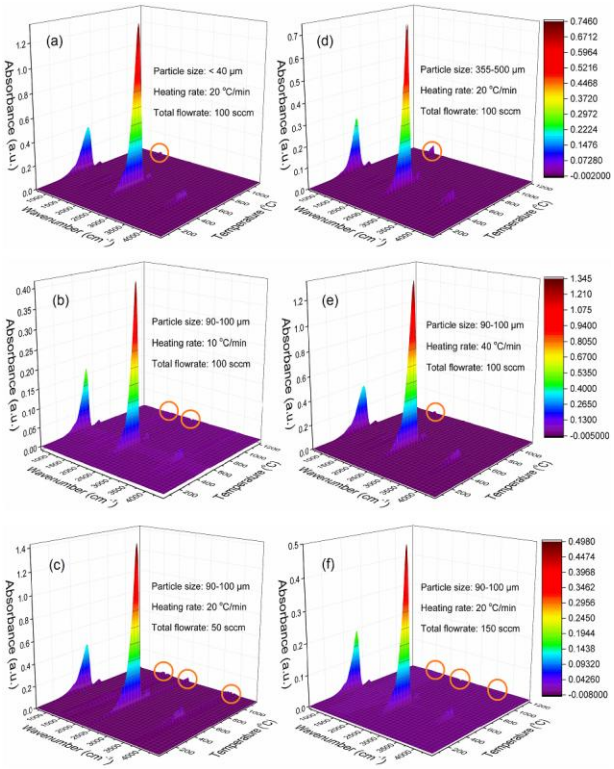

Fig. 8 FTIR spectra with different wavenumber and temperature.

range of 400-500 ℃, which is consistent with the rapid combustion temperature revealed in the MS analysis. Moreover, the peaks at 1375 and 3600 cm^{-1} correspond to SO_2 and H_2O, respectively. The differences marked in Fig. 8 indicate that less NO, SO_2 and H_2O are formed with smaller particle size, lower heating rate and larger total flowrate, which agrees well with the MS results.

The FTIR spectra at total range of wavenumber with different particle sizes, heating rates and total flowrates are shown in Fig. 9. It can be seen that the absorbance peaks moves slightly towards the higher wavenumber with the decrease of particle size, heating rate and total flowrate by comparison of the spectra curves.

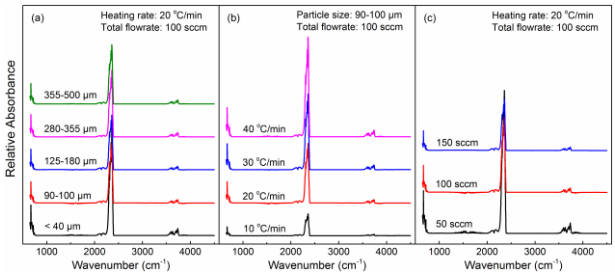

Fig. 9 FTIR spectra with different particle sizes, heating rates and total flowrates at 540 °C.

4. Conclusions

The combustion characteristic of Shenmu pulverized semi-coke (SSC) was systematically studied by an online TG-FTIR-MS system. The effect of particle size, heating rate and total flowrate on the characteristic temperatures, activation energy and products formation was revealed. The combustion products were accurately quantified by analysis of MS results. The rules of pollutant emission during combustion of SSC have been drawn. Five particle sizes ranging from 0-500 μm, four heating rates from 10-40 °C/min and three kinds of total flowrates (50 - 150 sccm) were used. The results indicate that the increase of total flowrates, decrease of particle sizes and heating rates lead to lower T_{ig}, T_{burn} and activation energy due to the larger amount of oxygen, bigger contact area of oxygen and sample surface with smaller particle size and more sufficient oxidation time at slower heating rate. Combining the qualitative and quantitative analyses of MS and FTIR results, lower concentrations of pollutant emissions such as NO and NO_2 were observed with slower heating rate and larger total flowrate. These results show some guidances to understand the SSC combustion process and finally control the pollutants from SSC combustion.

Acknowledgements

The authors thank the financial support from the the Strategic Priority Research Program of the Chinese Academy of Sciences (Grant No. XDA0703100) and the Recruitment Program of Global Youth Experts (Y41Z024BA1 and Y31Z061BA1). The authors also thank Mr. Kai Wei for his help in the experiments.

References

[1] L.B. Wang, X.Y. Bai, H.Q. Sun, S.Y. Wang, L.Y. Gong, Clean Coal Technology 17 (2011) 46.

[2] S.Y. Zhang, W.X. Wang, J.F. Lu, G.X. Yue, Y. Wang, Coal Combustion Facing the 21st Century (2003) 42.

[3] S.Y. Zhao, Coal science and Technology 35 (2007) 80.

[4] D.F. Liu, X.L. Liu, Coal Chemical Industry (2009) 26.

[5] F.B. Guo, Y.F. Zhang, G.J. Zhang, H.X. Zhao, J Power Sources 231 (2013) 82.

[6] P.R. Solomon, M.A. Serio, E.M. Suuberg, Prog Energ Combust 18 (1992) 133.

[7] Q.M. Yu, Y.J. Pang, H.G. Chen, North China Electric Power (2001) 9.

[8] J.P. Redfern, A.W. Coats, Nature Biotechnology 201 (1964) 68.

[9] H.D. Xia, K. Wei, Thermchimica Acta, accepted, DOI: 10.1016/j.tca.2014.12.019 (2014).

[10] Y. Wang, L. Wang, H.B. Shao, Clean-Soil Air Water 42 (2014) 1004.

[11] J.L. Yu, J.A. Lucas, T.F. Wall, Prog Energ Combust 33 (2007) 135.

[12] S. Kulasekaran, T.M. Linjewile, P.K. Agarwal, M.J. Biggs, Fuel 77 (1998) 1549.

[13] J.L. Yu, J. Lucas, T. Wall, G. Liu, C.D. Sheng, Combust Flame 136 (2004) 519.

[14] M.S. Nyathi, M. Mastalerz, R. Kruse, Int J Coal Geol 118 (2013) 8.

[15] L.M. Lu, C.H. Kong, V. Sahajwalla, D. Harris, Fuel 81 (2002) 1215.

[16] A.K. Sadhukhan, P. Gupta, R.K. Saha, Fuel Process Technol 90 (2009) 692.

[17] I. Kulaots, I. Aarna, M. Callejo, R.H. Hurt, E.M. Suuberg, P Combust Inst 29 (2002) 495.

[18] M.J.G. Alonso, A.G. Borrego, D. Alvarez, A. Menendez, Fuel Process Technol 69 (2001) 257.

[19] Y.H. Li, G.Q. Lu, V. Rudolph, Chem Eng Sci 53 (1998) 1.

[20] T. Ahamad, S.M. Alshehri, J Hazard Mater 199 (2012) 200.

[21] S. Silvera, J Anal Appl Pyrol 104 (2013) 95.